Systematic study of generalized flux phases

Franco Nori
Physics Department, University of Michigan, Ann Arbor, Michigan 48109-1120

Benoit Douçot and R. Rammal
Centre de Recherches sur les Très Basses Températures (CRTBT), Centre National de la Recherche Scientifique, Boîte Postale No. 166X, 38042, Grenoble CEDEX, France

(Received 22 August 1990; revised manuscript received 28 January 1991)

By using a mean-field Hartree-Fock treatment, models of strongly correlated fermions on a square lattice are reduced to the problem of fermions propagating in a magnetic field. We compute the kinetic energy of the Fermi sea for any value of the fermion density, magnetic flux, and frustration. From these we obtain, among other things, the optimal flux associated with the global energy minimum and the location of the local energy minima. Every cusp corresponds to an integer number of filled Landau levels, and the minimum-energy cusp corresponds to the one-level case. The breaking of time-reversal symmetry, when the diagonal coupling is turned on, produces a family of asymmetric cusps around $\Phi=\Phi_0/2$, in the one-particle energy. We use perturbation theory, valid for low fermion density, in order to analyze quantitatively the behavior of the cusplike energy minima; these minima are due to the Landau-level structure when the flux is close to a rational value. We have derived a phase diagram indicating regions of similar behavior and the points that exhibit anomalous dispersion induced by frustration.

I. INTRODUCTION

Recently, there has been much interest in the strong on-site repulsion limit of the two-dimensional Hubbard model on a square lattice.[1,2] In particular, various mean-field theories have been proposed to model the dynamics of a doped quantum antiferromagnet.[2] One of the main features of these theories is to treat the spin degrees of freedom with spin-$\frac{1}{2}$ fermions even in the vicinity of the metal-insulator transition, by contrast to the more traditional spin-wave approach to quantum antiferromagnets. In order to minimize the magnetic energy, the system self-consistently generates an effective magnetic flux, corresponding to half a flux quantum per plaquette for a half-filled square lattice. This is the flux phase discussed by Kotliar[3] and Affleck and Marston.[4]

More recently, it has been suggested that this approach can be generalized to the case of finite doping.[5] More precisely, it has been argued that the optimal effective flux should vary linearly with the doping as $\Phi=\pi(1-\delta)$, where δ is the hole concentration and Φ is the effective flux per plaquette.

These flux phases appear in a natural way in variational approaches studied by different groups.[6-11] The corresponding wave functions are obtained by filling a Fermi sea of electrons with the eigenstates of a noninteracting tight-binding Hamiltonian on the square lattice in the presence of a uniform magnetic field. Then a Gutzwiller projection is performed in order to eliminate the doubly occupied sites. The Hamiltonian we refer to is the widely studied (t-J) model on a two-dimensional square lattice, defined by

$$H=-t\sum_{\langle i,j\rangle}(1-n_{i-\sigma})c_{i\sigma}^{\dagger}c_{j\sigma}(1-n_{j-\sigma})+J\sum_{\langle i,j\rangle}(\mathbf{S}_i\cdot\mathbf{S}_j-\tfrac{1}{4}n_in_j)\ . \tag{1}$$

Here, the $c_{i\sigma}^{\dagger}$ operators are the bare electron-creation operators. Furthermore, H is restricted to the subspace where no doubly occupied sites are allowed, namely, $\sum_\sigma c_{i\sigma}^{\dagger}c_{i\sigma}\le 1$.

In order to calculate the average energy of these flux-state wave functions, several approaches have been proposed. One relies on the Gutzwiller approximation in order to calculate expectation values of the hopping terms in a state with no double occupancy.[7] The other line of approach involves a Hubbard-Stratonovich decoupling of both the hopping and the magnetic terms. This type of mean-field theory becomes exact in the large-N_f limit, where N_f is the number of different types of fermions.[8,9]

It has been shown that both methods give qualitatively the same estimate for the ground-state energy of these flux phases.[8,9] The results can be summarized as follows. Let us consider the mean-field effective tight-binding Hamiltonian

$$H_{\mathrm{MF}}=-\sum_{\langle i,j\rangle}e^{i\phi_{i,j}}c_i^{\dagger}c_j\ . \tag{2}$$

Here $\phi_{i,j}$ is related to a self-consistent vector potential $\mathbf{A}$ by

$$\phi_{i,j}=\frac{e}{\hbar}\int_i^j\mathbf{A}\cdot d\boldsymbol{l}\ . \tag{3}$$

Equation (2) implicitly assumes that the hopping amplitudes $|\langle c_{i\sigma}^{\dagger} c_{j\sigma}\rangle|$ do not depend on the link between sites i and j. In fact, at half filling, it has been shown that this large-N mean-field theory is unstable towards dimerization.[10] At finite doping, fixed dimers would prevent the motion of holes, and we expect that the hopping term then stabilizes a phase with uniform hopping amplitudes.

For a given doping δ, the number of fermions with a given type is $M=(N/2)(1-\delta)$. This comes from the fact that at half filling, the constraint is $\sum_{\alpha=1}^{N_f} c_{i\alpha}^{\dagger} c_{i\alpha}=N_f/2$. In the presence of holes, the constraint becomes $\sum_{\alpha=1}^{N_f}(c_{i\alpha}^{\dagger} c_{i\alpha}+b_i^{\dagger} b_i)=N_f/2$, where $b_i^{\dagger}$ creates a hole at site i.

Let us denote by ε_i the one-particle eigenvalues of H_{MF}, and define

$$\chi=-\frac{1}{N}\sum_{i=1}^{M}\varepsilon_i \ , \tag{4}$$

$$Q=-\min\{\varepsilon_i\} \ . \tag{5}$$

The mean-field free energy is then given by[8]

$$\frac{F}{NN_f}=-\frac{1}{8}(J\chi^2+t\delta Q\chi) \ . \tag{6}$$

This free energy is a function of the effective flux configuration through the set of variables $\{\phi_{i,j}\}$ and has to be minimized. Assuming a uniform magnetic flux Φ per plaquette reduces the problem to the evaluation of $\chi(\Phi)$ and $Q(\Phi)$.

The problem of free particles hopping on a two-dimensional (2D) square lattice in the presence of a uniform flux has been studied in great detail. The spectrum $\varepsilon_i(\Phi)$ has been calculated by Hofstadter,[12] and exhibits a rich self-similar structure. The edge of the spectrum $Q(\Phi)$, which enters in the expression of the hopping term, has been known since then. However, the quantity $\chi(\Phi)$, which is the energy of the Fermi sea with M particles, has been investigated only recently, in connection with the flux phases of the t-J model. As Eq. (6) shows, $\chi(\Phi)$ is involved in the expression of the magnetic energy.

In this paper we investigate the flux dependence of the ground-state energy $\chi(\Phi)$ of the Hamiltonian $H(\Phi)$ on a square lattice as a function of the particle density. We confirm the suggestion[5] that, for the unfrustrated case, $\chi(\Phi)$ is a minimum for $\Phi=\pi(1-\delta)$, which corresponds to one flux quantum per spinless fermion. We then study the effects of frustration on the flux dependence of the energy. This is done by considering the contributions coming from the next-nearest neighbor and third-nearest neighbor terms.

II. FERMI-SEA GROUND-STATE ENERGY FOR ARBITRARY FILLINGS AND FIELDS

The Hamiltonian we will consider here has the form

$$H=t_1\sum_{\langle i,j\rangle} c_i^{\dagger} c_j e^{i\phi_{i,j}}+t_2\sum_{\langle i,k\rangle} c_i^{\dagger} c_k e^{i\phi_{i,k}} +t_3\sum_{\langle i,l\rangle} c_i^{\dagger} c_l e^{i\phi_{i,l}}+\mathrm{H.c.} \ , \tag{7}$$

where $\langle i,j\rangle$ refers to a sum over the nearest-neighbor sites of a square lattice and the sum of $\phi_{i,j}$ along any closed contour gives the flux of the magnetic field through the enclosed area. The subindices k and l in the above equation refer to the second- and third-nearest neighbors of site i. Without loss of generality, t_1 will be set equal to 1 and t_2 will be positive. Since we are interested in the effects of frustration, we will focus on the case $t_3>0$ ($t_3<0$ does not add frustration to the system).

We have numerically diagonalized this general tight-binding problem with first-, second-, and third-nearest-neighbor couplings for lattices of various sizes, up to 30×30. The specific form of the gauge link used here is given by

$$\phi_{i,j}=\frac{2\pi}{\Phi_0}\int_i^j \mathbf{A}\cdot d\boldsymbol{l}=\pi(x_i+x_j)(y_j-y_i)\Phi \ ,$$

where (x_j,y_j) are the coordinates of site j, and Φ is the flux per elementary square plaquette in units of the flux quantum Φ_0. We calculate the ground-state energy $E(\Phi)$ for a fixed number $M=(N/2)(1-\delta)$ of particles by summing the first M energy eigenvalues. The total ground-state energy versus magnetic flux Φ per elementary square plaquette for several different filling factors is shown in Fig. 1. We have computed this quantity for every filling factor and about 200 values of the magnetic flux. Consequently, we are able to find the exact location of the global and local minima of the total energy with

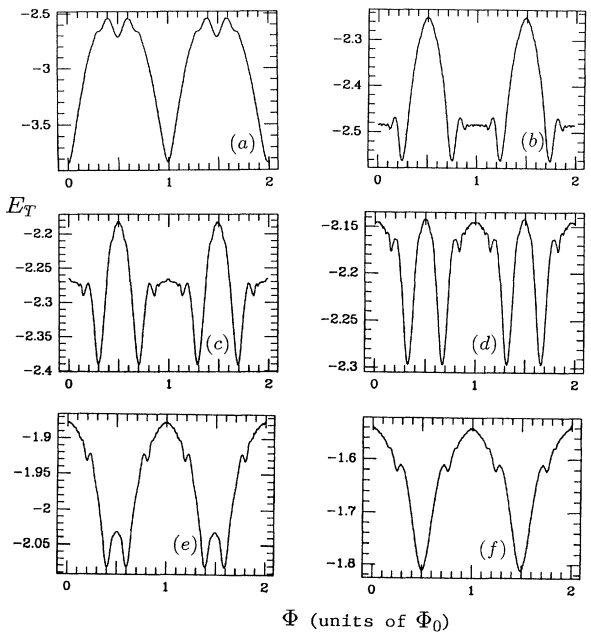

FIG. 1. Unfrustrated case: Fermi-sea total ground-state energy vs magnetic flux per unit cell for a 10×10 square lattice. The filling factors for fermions are equal to (a) 1/100 (i.e., one fermion), (b) 1/4, (c) 0.3, (d) 1/3, (e) 2/5, and (f) 48/100 (i.e., slightly below half filling). The minima become sharper for increasing system size. See, for instance, the results for a 20×20 lattice in Fig. 2.

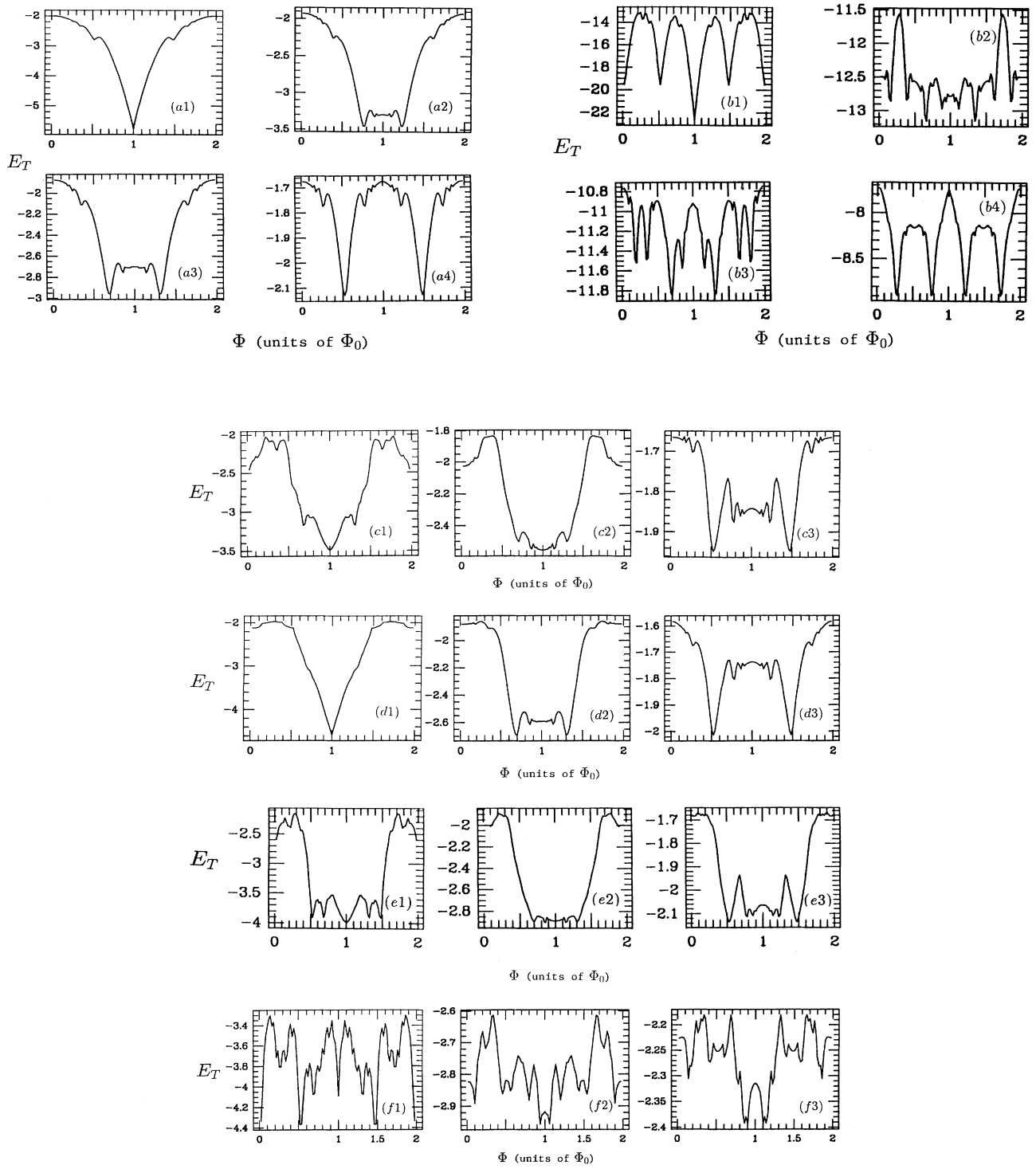

FIG. 2. Frustrated case: Fermi-sea total ground-state energy vs magnetic flux per unit cell for a 20×20 square lattice, obtained through exact diagonalization. The filling factors are (from top left to right, row by row) 1/400 (top left frame), 1/4 (top right), 1/3 (bottom left), and slightly below half filling, 198/400 (bottom right). The values of the (t_2,t_3) parameters are equal to (a) $(t_2,t_3)=(1/2,0)$, (b) large t_2 limit: (5,0). From now on, the filling factors are the following: 1/400, i.e., one fermion (left), 1/3 (center), and slightly below half filling, 198/400 (right). The different cases shown are (c) $(t_2,t_3)=(1/4,3/8)$, boundary $C\cap D\cap B\cap E$, (d) $(t_2,t_3)=(\sqrt{2}/4,\sqrt{2}/8)$, very anomalous case: flat dispersion, (e) (1/2, 1/2), (f) (1/10, 1), region D, limit case for large t_3, and $t_2\neq0$. Other limiting cases analyzed in detail (but not shown in the figures) are the following: (i) $(1/4,\sqrt{2}/8)$, which lies at the boundary $A\cap C$, (ii) (1/5, 1/5), which is a marginal case with a k^4 dispersion, (iii) (1,5), which is a limit case for large t_3, and $t_2\neq0$, (iv) (5,1), which is a limit case for large t_2, and $t_3\neq0$.

TABLE I. Ground-state degeneracies of $\Phi=1/2$ and $\Phi=1$ in each of the regions shown in Fig. 6.

Region	Ground state for $\Phi=2\pi$	Ground state for $\Phi=\pi$
A	$\mathbf{k}=(\pi,\pi)$	$\mathbf{k}=(0,0)$ and $\mathbf{k}=(\pi,0)$
B	$\mathbf{k}=(\pi,\pi)$	$\mathbf{k}=(\pm\pi/2,\pi/2)$
C	$\mathbf{k}=(\pi,\pi)$	$\mathbf{k}=(\pm\alpha,\pm\alpha)$ or $\mathbf{k}=(\pm(\pi-\alpha),\pm\alpha)$
D	$\mathbf{k}=(\pm k_0,\pm k_0)$	$\mathbf{k}=(\pm\alpha,\pm\alpha)$ or $\mathbf{k}=(\pm(\pi-\alpha),\pm\alpha)$
E	$\mathbf{k}=(\pm k_0,\pm k_0)$	$\mathbf{k}=(\pm\pi/2,\pi/2)$
	$\cos k_0=-\dfrac{1}{4t_3-2t_2}$	$\sin^2\alpha=\dfrac{1}{4t_2^2}\left[1-2t_3\left[\dfrac{1-8t_2^2}{4t_3^2-t_2^2}\right]^{1/2}\right]$

high accuracy. Figure 1, corresponding to the $t_2=t_3=0$ unfrustrated case, exhibits two prominent features: (i) The ground-state energy shows a global minimum as a function of the flux exactly at plus or minus one flux quantum per particle, $\Phi=x$ (modulo one flux quantum per plaquette) where $x=M/N$ is the electronic density. (ii) A set of harmonics is observed: There are local energy minima at $\Phi=x/m_1+m_2/m_1$, where m_1 and m_2 are arbitrary integers. It is important to point out that, away from half-filling, the Fermi energy at one flux quantum per particle lies in the biggest gap of the spectrum, which in the continuum limit is equivalent to the first Landau gap. The presence of the lattice is crucial to lift the degeneracy between fluxes corresponding to an integer number m of filled Landau levels ($\Phi/\Phi_0=x/m$). In the continuum, the energy has cusplike minima for $\Phi=x/m$, with the same energy as in the absence of magnetic field.

This lattice effect is quite striking, and is responsible for the stabilization of flux phases at large enough J/t, in the mean-field approach to the $t-J$ model. Because of its importance, we investigated this effect in the presence of frustration. Other studies, focusing on the case $t_2=t_3=0$ (i.e., no competing interactions) can be found in Ref. 11, while $1/S$ expansions and Lanczos studies of frustrated lattices can be found in Ref. 13. Results for various values of t_2 and t_3, and for several fixed sets of densities are shown in Fig. 2. The $E(\Phi)$ have been calculated for $0\le\Phi\le 2\Phi_0$, since in the presence of t_2 the spectrum is periodic as a function of Φ with the period $2\Phi_0$ instead of Φ_0 for the unfrustrated case. Several striking features are present in several of the plots in Figs. 2–6 and Tables I and II. For instance, the $(t_2,t_3)=(\sqrt{2}/4,\sqrt{2}/8)$ case has an anomalous flat dispersion, to be described below. Another anomalous example is the $(t_2,t_3)=(\frac{1}{2},\frac{1}{2})$ case with a k^4 *marginal* dispersion. Many of the plots in the $t_2\neq 0$, $t_3\neq 0$ regime were chosen precisely because they are located at boundaries in the t_2-t_3 plane. In them, the low-energy dispersion becomes *marginal* because the k^2 term vanishes at either $\Phi=1/2$ or $\Phi=1$.

When t_3 remains equal to zero, the one-particle ground state is reached for $\Phi=\Phi_0$. This comes from the fact that the one-particle spectrum for $\Phi=0$ is given by

$$\varepsilon(\mathbf{k})=2t_1(\cos k_x+\cos k_y)+4t_2\cos k_x\cos k_y \quad (\Phi=0)\ ,$$

$$\varepsilon(\mathbf{k})=2t_1(\cos k_x+\cos k_y)-4t_2\cos k_x\cos k_y \quad (\Phi=\Phi_0)\ .$$

The ground state is then $k=(\pi,\pi)$ for $\Phi=\Phi_0$. Increasing x leads to two cusplike minima for $E(\Phi)$, corresponding to $\Phi=\Phi_0(1\pm x)$. This behavior is quite similar to the pure t_1 case. However, when t_2/t_1 becomes large, this minimum disappears, and only the cusps at $\Phi=\Phi_0(1\pm x/m)$, $m\ge 2$ remain at $t_2\to\infty$. In this limit, the square lattice can be decomposed in two interpenetrating uncoupled sublattices, each having only nearest-neighbor hopping amplitudes, and a flux equal to 2Φ per elementary plaquette. Then, $E(\Phi)$ becomes periodic with the period $\Phi_0/2$, and around these values of the flux the cusplike minima are given by $\Delta\Phi=\Phi_0 x/2$. This behavior is indeed observed very clearly for $t_2=5$ and larger. The same figure shows that the local minima which are created around $\Phi=\Phi_0$ do not remain absolute

TABLE II. Location in the t_2-t_3 plane for all the systems studied in detail.

t_2	t_3	Region
$\frac{1}{10}$	0	A
$\frac{1}{4}$	0	A
0.49	0	A
1	0	B
2	0	B
5	0	B
10	0	B
$\frac{1}{5}$	$\frac{1}{5}$	C
$\frac{1}{2}$	$\frac{1}{2}$	$B\cap E$
$\frac{1}{10}$	1	D
$\frac{1}{4}$	$\frac{\sqrt{2}}{8}$	$A\cap C$
$\frac{1}{4}$	$\frac{3}{8}$	$C\cap D\cap B\cap E$
$\frac{\sqrt{2}}{4}$	$\frac{\sqrt{2}}{8}$	$A\cap B\cap C$
1	1	E
5	1	B
1	5	E

minima at large density x. For instance, at $x=\frac{1}{4}$, the absolute minimum originates from $\Phi=\Phi_0/2$. Needless to say, large values of t_2/t_1 and t_3/t_1 are not physical. However, these limits are helpful to understand the structure observed at smaller values of t_2 and t_3. From our graphs, for $t_2 \geq 2$, a sharp cusp appears at $\Phi=\Phi_0/2$, in the one-particle energy. Upon doping, this cusp generates a series of local cusps, which have qualitatively the same features as the $\Phi=\Phi_0$ family. However, we should stress that these minima are asymmetric around $\Phi=\Phi_0/2$ in contrast to what is found around $\Phi=\Phi_0$. The origin of this asymmetry comes from *the breaking of time-reversal symmetry* at $\Phi=\Phi_0/2$, when the t_2 coupling is switched on. Furthermore, the position of these cusps is given by $\Phi=(\Phi_0/2)(1\pm x/m)$, to be compared with $\Phi=\Phi_0(1\pm x/m)$ for the vicinity of Φ_0.

As will be shown in Sec. III, this different behavior comes from the fact that the density of states in a Landau level for $\Phi\sim\Phi_0/2$ is twice the corresponding value for $\Phi\sim\Phi_0$. The local minimum corresponds in both cases to filling exactly one Landau level, but in terms of the densities, this leads to reducing the flux variations by a factor 1/2 around $\Phi=\Phi_0/2$.

If t_3 is now turned on, we observed that the $E(\Phi)$ curves become flatter around $\Phi=\Phi_0$. This is the result of frustration, as can be seen from the dispersion relation for $\Phi=\Phi_0$:

$$\varepsilon(\mathbf{k})=2(\cos k_x+\cos k_y)-4t_2\cos k_x\cos k_y + 2t_3(\cos 2k_x+\cos 2k_y)\ .$$

Here, the first two terms compete with the t_3 contribution. If $t_3<\frac{1}{4}+t_2/2$, the one-particle ground state remains nondegenerate at $\mathbf{k}=(\pi,\pi)$. When $t_3>1/4+t_2/2$, the ground state becomes fourfold degenerate at $\mathbf{k}=(\pm k_0,\pm k_0)$, with k_0 given by

$$\cos k_0=\frac{-1}{4t_3-2t_2}\ .$$

For $t_3=\frac{1}{4}+t_2/2$, the dispersion of the low-lying states is *marginal*, with $\varepsilon(\mathbf{k})\sim k^4$, whereas $\varepsilon(\mathbf{k})\sim k^2$ elsewhere.

When Φ is slightly different from Φ_0, the effect of this marginal dispersion is quite striking and is illustrated by the $t_2=t_3=\frac{1}{2}$ case. For this model, $E(\Phi)$ *remains nearly flat around* $\Phi=\Phi_0$ up to $x=\frac{1}{3}$, *in spite of the presence of local cusps.*

When t_3 is further increased, Fig. 2 shows that the absolute minimum of $E(\Phi)$ is at $\Phi=\Phi_0/2$ for one particle and moves with x, according to $\Phi=\Phi_0(1+x)/2$. Note that $\Phi=\Phi_0(1-x)/2$ is a local minimum with a higher energy. Here again, it is a manifestation of broken time-reversal symmetry at $\Phi=\Phi_0/2$. The behavior of $E(\Phi)$ around $\Phi=\Phi_0/2$ is quite analogous to what is observed for $t_3=0$ and $t_2>1$. In the limit where t_3 is large compared to t_2 and t_1, the model becomes equivalent to four interpenetrating uncoupled square sublattices with a flux per plaquette equal to 4Φ. Then, the period of $E(\Phi)$ is $\Phi_0/4$, and in this limit, the location of the cusps is given by $\Phi=\Phi_0(p\pm x)/4$, where $p=0,1,2$, or 3. As a result, the cusps corresponding to $\Phi=\Phi_0(1\pm x/m)/2$ at finite t_3 have to disappear progressively for $m=1$. This is clearly observed in Fig. 2 for the large-t_3 limit case $(t_2,t_3)=(1,5)$. Also, compare the $x=1/6$ concentration between the figures corresponding to $(t_2,t_3)=(1,1)$ and $(t_2,t_3)=(1,5)$.

To summarize these numerical results, we find a large variety of behaviors for $E(\Phi)$, as t_2 and t_3 are varied. However, some major features remain unchanged. More precisely, $E(\Phi)$ always exhibits cusplike minima which position moves linearly as a function of the fermion density x. Frustration may induce a competition between different local minima. Indeed, most of the qualitative features can be understood by first considering the local minima of $E(\Phi)$ for one particle only. These occur for simple values of Φ such as 0, Φ_0, $\Phi_0/2$, $3\Phi_0/2$, and other rational fractions of Φ_0. Changing Φ slightly away from these values gives a Landau-level structure for the one-particle spectrum. As will be shown in Sec. III, such a spectrum leads to a family of cusps which move away from the original flux value as x is increased. These cusps correspond to an integer number of filled Landau levels, the minimum being for one level exactly.

III. FERMI-SEA GROUND-STATE ENERGY: PERTURBATION THEORY

Let us now turn to a quantitative analysis, to describe the behavior of the cusplike minima at low densities x. The cusps originate from the Landau-level structure when Φ/Φ_0 is close to a rational value p/q. For $\Phi/\Phi_0=p/q$, the spectrum is split in q subbands. Then, for Φ/Φ_0 slightly away from p/q, each subband generates a secondary Landau-level structure, and the construction of the complete spectrum obeys this recursive scheme. It has been shown[14] how to set up a semiclassical approach to calculate the Landau-level spectrum around any rational value of the flux. Here, we compare the results obtained in this formalism with the exact diagonalization results.

For the sake of clarity, let us first concentrate on the nearest-neighbor case ($t_2=t_3=0$) at small fields. From now on, Φ_0 will be set equal to unity. The tight-binding Schrödinger equation in the usual Landau gauge leads to Harper's equation[12]

$$\varepsilon g(n)=-2\cos(\gamma n+k_x)g(n)-g(n-1)-g(n+1)\ .$$

Here $\gamma=2\pi\Phi$. In the low-field regime, the magnetic length scale is proportional to $\gamma^{-1/2}$, so we can take a continuum limit. This is achieved by expanding the cosine in the power series around its minimum. Choosing the origin so that $k_x=0$, one obtains

$$(\varepsilon+4)g(n)=\gamma^2n^2g(n)-g''(n)+[g''(n)-g(n-1) -g(n+1)+2g(n)]-\tfrac{1}{12}\gamma^4n^4g(n)\ .$$

We now introduce a reduced variable $x=n\gamma^{1/2}$ and define F such that $g(n)=F(n\gamma^{1/2})=F(x)$.

In the continuum limit, the lattice difference operators

become differential operators and expanding to order γ^2, the Harper equation becomes

$$\frac{\varepsilon+4}{\gamma}F(x)=x^2F(x)-F''(x)-\frac{1}{12}\gamma[F''''(x)+x^4F(x)] .$$

This is the Schrödinger equation for a perturbed harmonic oscillator. The spectrum is obtained to the order γ^2 by nondegenerate perturbation theory. This leads to the following Landau level spectrum:

$$\varepsilon_n=-4+(2n+1)\gamma-\frac{1}{16}\gamma^2[(2n+1)^2+1]+0(\gamma^3) . \tag{8}$$

A similar spectrum is actually found in the presence of frustration, in the vicinity of $\Phi=1$. It is completely determined to order γ^2 from the dispersion relation up to order k^4 for the low-lying states in the absence of flux. Assuming that near its minimum at $\mathbf{k}_0$, $\varepsilon(k_x,k_y)$ has the following Taylor expansion in $\mathbf{k}-\mathbf{k}_0=(k_x,k_y)$:

$$\varepsilon(k_x,k_y)=\varepsilon(\mathbf{k}_0)+\frac{\omega}{2}(k_x^2+k_y^2)+O(|\mathbf{k}|^3) . \tag{9}$$

It has been shown[14] that for small fields ($\gamma \ll 1$), the Landau-level spectrum is given by

$$\varepsilon_n=\varepsilon(\mathbf{k}_0)+\frac{\omega\gamma}{2}(2n+1)+\frac{\gamma^2}{64}\Delta^2\varepsilon(k_0)[(2n+1)^2+1]$$
$$-\frac{\gamma^2}{288\omega}[9(3n^2+3n+1)|\Delta\partial\varepsilon(\mathbf{k}_0)|^2$$
$$+(3n^2+3n+2)|\partial^3\varepsilon(\mathbf{k}_0)|^2]+O(\gamma^3) , \tag{10}$$

where

$$\partial=\frac{\partial}{\partial k_x}-i\frac{\partial}{\partial k_y} \text{ and } \Delta=\frac{\partial^2}{\partial k_x^2}+\frac{\partial^2}{\partial k_y^2} .$$

In the presence of t_2 and t_3, two situations have to be distinguished.

(a) $t_3<\frac{1}{4}+2t_2$. $\mathbf{k}=(\pi,\pi)$ is the nondegenerate ground state at $\Phi=1$. The low-lying states are then given by

$$\varepsilon(k_x,k_y)=-4-4t_2+4t_3+\gamma(1+2t_2-4t_3)(k_x^2+k_y^2)$$
$$-t_2k_x^2k_y^2-\left[\frac{1}{12}+\frac{t_2}{6}-\frac{4}{3}t_3\right](k_x^4+k_y^4) . \tag{11}$$

The corresponding Landau-level spectrum is

$$\varepsilon_n=-4-4t_2+4t_3+\gamma(1+2t_2-4t_3)(2n+1)$$
$$-\frac{1}{16}\gamma^2(1+4t_2-16t_3)[(2n+1)^2+1] . \tag{12}$$

(b) $t_3>\frac{1}{4}+2t_2$. The ground state is fourfold degenerate, with $\mathbf{k}=(\pm k_0,\pm k_0)$, and $\cos k_0=-1/(4t_3-2t_2)$. Expanding around $\mathbf{k}=(\eta_x k_0,\eta_y k_0),\eta_x=\pm1,\eta_y=\pm1$, we find

$$\varepsilon(k_x,k_y)=-4t_3-\frac{1}{2t_3-t_2}+4t_3(\sin^2k_0)(k_x^2+k_y^2)-4t_2(\sin^2k_0)\eta_x\eta_yk_xk_y+2t_3\sin(2k_0)(\eta_xk_x^3+\eta_yk_y^3)$$
$$-t_2\sin(2k_0)(\eta_xk_xk_y^2+\eta_yk_x^2k_y)+t_3(1-\tfrac{7}{3}\sin^2k_0)(k_x^4+k_y^4)-t_2(\cos^2k_0)k_x^2k_y^2+\tfrac{2}{3}t_2(\sin^2k_0)\eta_x\eta_y(k_x^3k_y+k_xk_y^3) . \tag{13}$$

The associated Landau spectrum is detailed in the Appendix. Figure 3 shows a few examples of Landau-level spectra obtained from the second-order perturbation theory presented above. We have plotted the first nine Landau levels, each one labeled by n (where $n=0,1,2,\ldots,8$) and small values (up to 0.1) of the magnetic field. Our small parameters, as the reader will recall, are the magnetic field and the fermion density. From the figures it is clear that the larger the value of n, the smaller is the magnetic field for which perturbation theory becomes inapplicable. For instance, let us focus on Fig. 3(a), corresponding to the $(t_2,t_3)=(0,0)$ case. The $n=0$ Landau level, starting at $E=-4$ for zero field, is a straight line. When n grows, the levels bend and eventually go downwards. This trend becomes more pronounced for the large-t_2-limit case, $(t_2,t_3)=(2,0)$, shown in Fig. 3(b). The other examples that follow behave differently because, as noted below, they are somewhat anomalous. For instance, Fig. 3(d), corresponding to $(t_2,t_3)=(1/2,1/2)$, is a marginal case because *the dispersion relation goes like k^4 instead of k^2*. Also Fig. 3(c) corresponds to a *flat dispersion*. Figures 3(e) and 3(f) correspond to points that belong to "boundary lines" between the regions $A\cap C$ and $C\cap D\cap B\cap E$, respectively. These regions correspond to the different possible behaviors of the dispersion relation at low energy for $\Phi=1/2$ and $\Phi=1$. These regions, shown in Fig. 6 and Tables I and II, will be described below.

Let us now consider a system with a finite density of fermions x. For a small field, $\gamma \ll 1$, the Fermi sea is obtained by filling ν Landau levels. The total number of states in a given Landau level is proportional to the number of flux quanta in the system. As a result, $x=\nu\Phi=\nu\gamma/2\pi$. Let us denote by m the number of Landau levels which are completely filled ($m\le\nu<m+1$). The energy of the Fermi sea is obtained by

$$\frac{1}{N}E(\Phi,x)=\frac{\gamma}{2\pi}\left[\sum_{n=0}^{m-1}\varepsilon_n(\Phi)\right]+\frac{\gamma}{2\pi}(\nu-m)\varepsilon_m(\Phi) .$$

Using the previous expression for $\varepsilon_n(\Phi)$ and reexpressing γ as a function of x and ν, this leads to

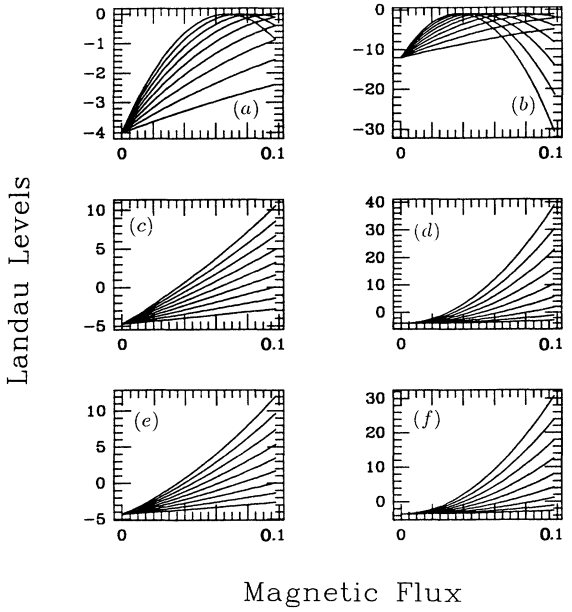

FIG. 3. Landau-level spectrum for a square lattice in a uniform and small magnetic field obtained from second-order perturbation theory. Frustration is induced by the second- and third-nearest neighbor couplings. The values of n, labeling different Landau levels, shown are $n=0,1,2,\ldots,8$, in ascending order. The values of the (t_2,t_3) parameters are equal to (a) (0,0), (b) (2,0), (c) $(\sqrt{2}/4,\sqrt{2}/8)$, (d) (1/2, 1/2), (e) $(1/4,\sqrt{2}/8)$, and (f) (1/4, 3/8).

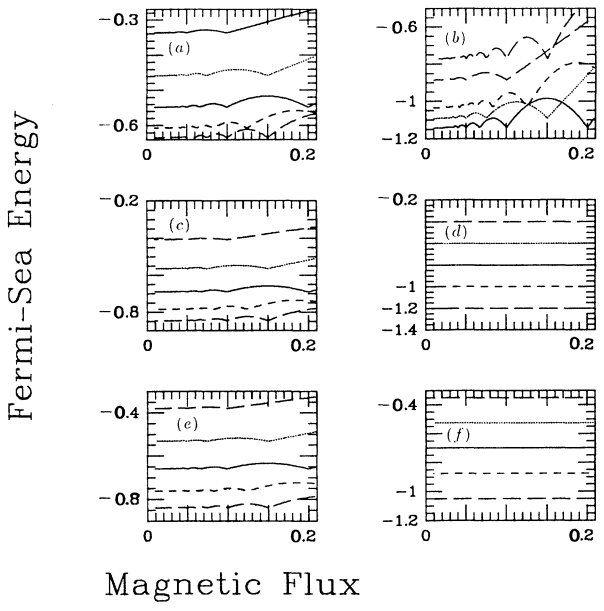

FIG. 4. Energy of a filled Fermi sea vs magnetic field obtained from perturbation theory, for the following fermion densities (from top to bottom): $x=0.1$, 0.15, 0.2, 0.25, and 0.3. Only (b) has a different ordering (from top to bottom at zero field): $x=0.3$, 0.1, 0.25, 0.15, and 0.2. Our choice of (small) fermion density and (small) filling factors is dictated by the fact that these are the small parameters of the perturbation. The values of (t_2,t_3) are the same as in Fig. 3.

$$\frac{1}{N}E(\Phi,x)=x\varepsilon_0+\omega\pi x^2\frac{[(m+1)^2-m^2](\nu-m)+m^2}{\nu^2}+\frac{\pi^2}{12}x^3\frac{m^3+[(m+1)^3-m^3](\nu-m)}{\nu^3}$$
$$\times\left[\Delta^2\varepsilon(0)-\frac{1}{6\omega}[9|\Delta\partial\varepsilon(0)|^2+|\partial^3\varepsilon(0)|^2]\right]+\frac{\pi^2}{24}\frac{x^3}{\nu^2}\left[\Delta^2\varepsilon(0)-\frac{1}{3\omega}|\partial^3\varepsilon(0)|^2\right]. \tag{14}$$

When the filling factor is an integer, $\nu=m$, the formula becomes

$$\frac{1}{N}E(\nu=m,x)=x\varepsilon_0+\omega\pi x^2+\frac{\pi^2}{12}x^3\left[\Delta^2\varepsilon(0)-\frac{1}{6\omega}[9|\Delta\partial\varepsilon(0)|^2+|\partial^3\varepsilon(0)|^2]\right]$$
$$+\frac{\pi^2}{24}\frac{x^3}{m^2}\left[\Delta^2\varepsilon(0)-\frac{1}{3\omega}|\partial^3\varepsilon(0)|^2\right], \tag{15}$$

where $\varepsilon_0=\varepsilon(0)=\varepsilon(\mathbf{k}_0)$. The last term lifts the degeneracy between different values of m, and, since $\Delta^2\varepsilon(0)$ is usually negative on a lattice, the minimum of $E(\nu=m,x)$ is obtained for $m=1$, in agreement with Anderson's conjecture.[5] The $E(\Phi,x)$ vs Φ curve exhibits a cusp at every integer filling factor m. More precisely,

$$\frac{1}{N}\frac{\partial E(\Phi,x)}{\partial\gamma}\bigg|^{+}=-\frac{\omega}{2}x-\frac{\pi}{24}x^2\left[3\Delta^2\varepsilon(0)-\frac{3}{2\omega}\left[3+\frac{1}{m}\right]\left|\Delta\partial\varepsilon(0)\right|^2-\frac{1}{6\omega}\left[3-\frac{1}{m}\right]\left|\partial^3\varepsilon(0)\right|^2\right], \tag{16}$$

$$\frac{1}{N}\frac{\partial E(\Phi,x)}{\partial\gamma}\bigg|^{-}=\frac{\omega}{2}x+\frac{\pi}{24}x^2\left[3\Delta^2\varepsilon(0)-\frac{3}{2\omega}\left[3-\frac{1}{m}\right]\left|\Delta\partial\varepsilon(0)\right|^2-\frac{1}{6\omega}\left[3+\frac{1}{m}\right]\left|\partial^3\varepsilon(0)\right|^2\right]. \tag{17}$$

These derivatives are taken at $\nu=m$. Therefore, the cusp is not symmetric. This is not readily visible on the figures, unless magnified. Figure 4 shows the energy of a filled Fermi sea, for five values of the filling factor, obtained from Eq. (14). The filling factors are (from top to bottom) $x=0.1$, 0.15, 0.2, 0.25, and 0.3. Only Fig. 4(b) has a different ordering (from top to bottom at zero field): $x=0.3$, 0.1, 0.25, 0.15, and 0.2. Our choice of (small) fer-

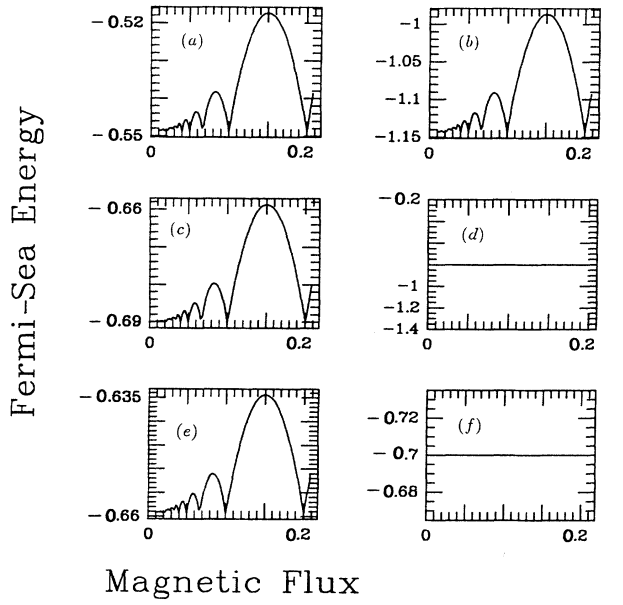

FIG. 5. Energy of a filled Fermi sea vs magnetic field obtained from perturbation theory. In order to observe better the cusplike structure, only one fermion density has been used: $x=0.2$. We use the same values of (t_2,t_3) and present them in the same order, as in Figs. 3 and 4.

mion density and (small) filling factors is dictated by the fact that these are the small parameters of the perturbation. In order to observe better the cusplike structure, the $x=0.2$ case is presented in Fig. 5. We use the same values of (t_2,t_3) and present them in the same order, as in Figs. 3 and 4.

Let us now briefly discuss the vicinity of $\Phi=1/2$. As for the $\Phi=1$ case, the behavior of $E(\Phi,x)$ around $\Phi=\frac{1}{2}$ for fixed x will depend on the one-particle spectrum for $\Phi=1/2$. This spectrum is given by

$$\varepsilon(k_x,k_y)=2t_3(\cos 2k_x+\cos 2k_y) -2(\cos^2 k_x+\cos^2 k_y+4t_2^2\sin^2 k_x\sin^2 k_y)^{1/2} , \tag{18}$$

where (k_x,k_y) belongs to the reduced Brillouin zone: $-\pi\le k_x\le\pi$ and $-\pi/2\le k_y\le\pi/2$.

We find three different regimes, in the (t_2,t_3) plane, for the ground state of the one-particle spectrum.

(1) $t_3<\min\left[\frac{\sqrt{2}}{8},\frac{\sqrt{2}}{4}-\frac{|t_2|}{2}\right]$:

Here $\mathbf{k}=(0,0)$ or $\mathbf{k}=(\pi,0)$ is a twofold-degenerate ground state.

(2) $t_3>\frac{1}{8t_2}-\frac{t_2}{2}$ and $t_2<\frac{\sqrt{2}}{4}$ or $t_3>\frac{\sqrt{2}}{4}-\frac{t_2}{2}$ and $t_2>\frac{\sqrt{2}}{4}$:

The ground state corresponds to $(k_x,k_y)=(\pm\pi/2,\pm\pi/2)$, which is twofold degenerate, since $k_y=\pi/2$ and $k_y=-\pi/2$ are the same state.

(3) $\frac{\sqrt{2}}{8}<t_3<\frac{1}{8t_2}-\frac{t_2}{2}$ and $t_2<\frac{\sqrt{2}}{4}$:

The ground state has an eightfold degeneracy. It is defined by

$$\sin^2 k_x=\sin^2 k_y =\frac{1}{4t_2^2}\left[1-2t_3\left[\frac{1-8t_2^2}{4t_3^2-t_2^2}\right]^{1/2}\right] .$$

The calculation of the low-lying Landau spectrum for $\Phi\sim 1/2$ is more complicated than for $\Phi\sim 1$, since here the unit cell is doubled because of the presence of half a flux quantum per cell.

As already discussed in the general description of the numerical results, each Landau level around $\Phi=1/2$ contains a number of states equal to $2|\Phi-1/2|N$. In the case of the Hofstadter spectrum this property is a direct consequence of the linear dependence of the integrated density of states on the flux.[15] For instance, the gap above the first Landau level, between $\Phi=1/3$ and $\Phi=1/2$, corresponds to $x=-2\Phi+1$. This implies that around $\Phi=1/2$, a Fermi sea with exactly m filled Landau levels corresponds to

$$\Phi=\tfrac{1}{2}\pm x/2m ,$$

by contrast to the previous

$$\Phi=1\pm x/m .$$

We should stress that a similar analysis[14] can be done in the neighborhood of any rational value $\Phi=p/q$. More precisely, a cusp in the $E(\Phi,x)$ vs x curve is expected when x and Φ are such that an integer number of subbands are filled. For $\Phi=p/q$, this corresponds to $x=n/q$, where n,p,q are integers. However, the cusps corresponding to larger values of q are more difficult to see numerically.

On Fig. 6 we have represented the regions in the t_2-t_3 space corresponding to the different possible behaviors of the dispersion relation at low energy, for $\Phi=1/2$ and $\Phi=1$. The results presented above sample these different cases. For convenience, Table I summarizes the ground-state degeneracies for $\Phi=1/2$ and $\Phi=1$ in each of the regions. Furthermore, Table II provides the location on the t_2-t_3 plane for all the systems studied. *In general, the low-energy dispersion becomes marginal* (i.e., the k^2 term vanishes) at either $\Phi=1/2$ or $\Phi=1$ *when a boundary is crossed.* An exception is the boundary between A and B, given by $t_3=\sqrt{2}/4-t_2/2$ and $t_2>\sqrt{2}/4$. Crossing this line, the ground state for $\Phi=1/2$ jumps from $\mathbf{k}=(0,0)$ to $\mathbf{k}=(\pm\pi/2,\pi/2)$, and the quadratic term in the dispersion relation remains finite.

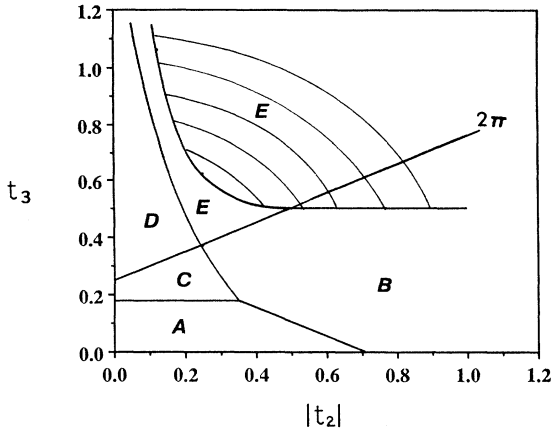

FIG. 6. Regions in the t_2-t_3 space corresponding to the different possible behaviors of the dispersion relation at low energy, for $\Phi=1/2$ and $\Phi=1$. The boundaries between regions of similar behavior $E(\Phi)$ are indicated. The shaded region ($t_3>1/8t_2+|t_2|/2$ and $t_3>1/2$) is where $\Phi=1/2$ is more stable for the one-fermion energy. Tables I and II complement the information presented in this figure.

In summary, through a mean-field Hartree-Fock treatment, we have studied the energetics of fermions confined to a two-dimensional square lattice. Our goal has been to compute the kinetic energy of the Fermi sea of the spinless fermions for any value of the fermion concentration, magnetic flux, and frustration. For the unfrustrated case, we confirm the suggestion[5] that the ground-state energy $\chi(\Phi)$ is a minimum for $\Phi=\pi(1-\delta)$, which corresponds to one flux quantum per spinless fermion. We then proceed to do a systematic study of frustration effects, coming from longer-range couplings, which modify the picture obtained for the unfrustrated case. These effects constitute the main focus of this work. We find that, in general, $E(\Phi)$ always exhibits cusplike minima, the position of which moves linearly as a function of the fermion density x. Frustration can induce a competition between different local minima. By first considering the local minima for one particle only, we can understand most of the qualitative features of $E(\Phi)$. These local minima occur at simple rational fractions of Φ_0, and when the flux slightly deviates from these values a one-particle Landau-level structure develops. It is precisely such a spectrum that generates a family of cusps that "move away" from the original flux value as x is increased. Every cusp corresponds to an integer number of filled Landau levels, and the minimum energy cusp corresponds to the one-level case. Furthermore, we use perturbation theory, valid for low fermion density x, in order to analyze quantitatively the behavior of the cusplike energy minima, which originate from the Landau-level structure when the flux is close to a rational value. If the flux is slightly away from a given rational value p/q, each of the q subbands generates a secondary Landau-level structure. We have derived a t_2-t_3 phase diagram indicating regions of similar behavior [i.e., *adiabatic continuations* can be performed with each region, preserving the $E(\Phi)$ structure] and the boundaries between them. We have studied several points belonging to those boundaries and found that anomalous behavior, induced by frustration, can occur.

This work confirms that the stabilization of a Fermi sea in the presence of uniform flux is intrinsically a lattice effect. A quite dramatic consequence of frustration is to modify the one flux quantum per particle rule for the optimal state, when t_2 and t_3 are large enough.

A natural interpretation for this rule is to say that if a one-flux-quantum flux tube is attached to the spinless fermions, they become hard-core bosons, which is expected to give the lowest possible kinetic energy at a given particle density. Treating these flux tubes in a mean-field approximation leads to a uniform field with precisely one flux quantum per particle.[16] The breakdown of this rule in the presence of a large frustration may indicate that the energy of a many-particle system exhibits then a quite complicated dependence as a function of the fractional statistics parameter. Another possibility is that approximating flux tubes by a uniform flux gives a poor estimate of the ground-state energy in the presence of frustration.

Our study suggests that some similarities exist between the geometric frustration and the one which is associated to a magnetic field. We think the results presented here give some idea about the rich variety of behaviors that can occur when these two sources of frustration are combined.

ACKNOWLEDGMENTS

This research has been supported in part by NSF Grant Nos. DMR-90-01502 and PHY89-04035. B.D. would like to thank I.T.P. Santa Barbara for support and hospitality, and the University of Michigan for hospitality.

APPENDIX

Here we will consider the Landau-level spectrum around $\Phi=1$, for $t_3>1/4+2t_2$. Let us first consider the following change of coordinates:

$$k_x=\frac{g^{-1}u+gv}{\sqrt{2}};\quad k_y=\frac{-g^{-1}u+gv}{\sqrt{2}};\quad g=\left[\frac{2t_3+t_2}{2t_3-t_2}\right]^{1/4}. \tag{A1}$$

This diagonalizes the quadratic part of the dispersion. Furthermore, in the quantum problem, k_x and k_y become operators which satisfy $[\mathbf{K}_x,\mathbf{K}_y]=i\gamma$. The transformation above implies that $[\mathbf{u},\mathbf{v}]=i\gamma$ as well. Before quantization (i.e., working with real numbers), one gets

$$\varepsilon(u,v)=-4t_3-\frac{1}{4t_3-t_2}+2\sin^2k_0(4t_3^2-t_2^2)^{1/2}(u^2+v^2)+\sqrt{2}t_3\sin 2k_0(3g^{-1}u^2v+g^3v^3)$$
$$+\frac{t_2}{\sqrt{2}}\sin 2k_0(g^{-1}u^2v-g^3v^3)+\frac{t_3}{2}\left[1-\frac{7}{3}\sin^2k_0\right](g^{-4}u^4+6u^2v^2+g^4v^4)$$
$$-\frac{t_2}{4}\cos^2k_0(g^{-4}u^4-2u^2v^2+g^4v^4)+\frac{t_2}{2}\sin^2k_0(-g^{-4}u^4+g^4v^4)\ . \tag{A2}$$

Here, we assumed $\eta_x=\eta_y=1$, since the spectrum is independent of η_x and η_y. Then, the Landau levels are given by Eq. (10), with

$$\omega=4\sin^2k_0(4t_3^2-t_2^2)^{1/2}\ , \tag{A3}$$

$$\Delta^2\varepsilon(0)=12t_3(1-\tfrac{7}{3}\sin^2k_0)(g^{-2}+g^2)^2-2t_2(3g^{-4}-2+3g^4)+t_2\sin^2k_0(18g^4-4-6g^{-4})\ , \tag{A4}$$

$$|\Delta\partial\varepsilon(0)|=|6\sqrt{2}t_3(g^{-1}+g^3)+\sqrt{2}t_2(g^{-1}-3g^3)||\sin 2k_0|\ , \tag{A5}$$

$$|\partial^3\varepsilon(0)|=\left|\sqrt{2}t_3(18g^{-1}-6g^3)+\frac{t_2}{\sqrt{2}}(6g^{-1}+6g^3)\right||\sin 2k_0|\ . \tag{A6}$$

[1] P. W. Anderson, Science **235**, 1196 (1987).

[2] For a recent review, see E. Manousakis, Rev. Mod. Phys. **63**, 1 (1991).

[3] G. Kotliar, Phys. Rev. B **37**, 3664 (1988).

[4] I. Affleck and J. B. Marston, Phys. Rev. B **37**, 3774 (1988); **39**, 11 538 (1989).

[5] P. W. Anderson, Physica Scripta **T27**, 60 (1989).

[6] Y. Hasegawa, P. Lederer, T. M. Rice, and P. B. Wiegmann, Phys. Rev. Lett. **63**, 907 (1989); G. Montambaux, *ibid.* **63**, 1657 (1989); P. W. Anderson, B. S. Shastry, and D. Hristopoulos, Phys. Rev. B **40**, 8939 (1989).

[7] P. Lederer, D. Poilblanc, and T. M. Rice, Phys. Rev. Lett. **63**, 1519 (1989); D. Poilblanc, Y. Hasegawa, and T. M. Rice, Phys. Rev. B **41**, 1949 (1990).

[8] J. Rodriguez and B. Douçot, Europhys. Lett. **11**, 451 (1990).

[9] F. Nori, E. Abrahams, and G. Zimanyi, Phys. Rev. B **41**, 7277 (1990).

[10] T. Dombre and G. Kotliar, Phys. Rev. B **39**, 855 (1989).

[11] J. P. Rodriguez and B. Douçot, Phys. Rev. B **42**, 8724 (1990); R. Rammal, J. Phys. (Paris) **46**, 1345 (1985); R. Rammal and J. Bellisard, Europhys. Lett. **13**, 205 (1990); E. Fradkin, Phys. Rev. Lett. **63**, 322 (1989); Phys. Rev. B **42**, 570 (1990); T. C. Hsu, *ibid.* **41**, 11 379 (1990); F. Nori and G. Zimanyi, Europhys. Lett. **16**, 397 (1991); T. M. Rice, in *High Temperature Superconductivity*, edited by K. Bedell *et al.* (Addison-Wesley, Reading, 1990), p. 302; D. Poilblanc, Phys. Rev. B. **41**, 4827 (1990); D. Poilblanc and Y. Hasegawa, *ibid.* **41**, 6989 (1990); Y. Hatsugai and M. Kohmoto, *ibid.* **42**, 8282 (1990); M. Kohmoto and Y. Hatsugai, *ibid.* **41**, 9527 (1990); Y. Hasegawa, Y. Hatsugai, M. Kohmoto, and G. Montambaux, *ibid.* **41**, 9174 (1990); S. Liang and N. Trivedi, Phys. Rev. Lett. **64**, 232 (1990); D. N. Sheng, Z. B. Su, and Lu Yu, Phys. Rev. B **42**, 8732 (1990); T. K. Lee and S. Feng, *ibid.* **38**, 11 809 (1988).

[12] D. R. Hofstadter, Phys. Rev. B **14**, 2239 (1976).

[13] P. Chandra and B. Douçot, Phys. Rev. B **38**, 9335 (1988); P. Chandra, P. Coleman, and A. Larkin, Phys. Rev. Lett. **64**, 88 (1990); E. Dagotto and A. Moreo, Phys. Rev. B **39**, 4744 (1989); Phys. Rev. Lett. **41**, 2313 (1990); F. Figueirido, A. Karlhede, S. Kivelson, S. Sondhi, M. Rocek, and D. S. Rokhsar, Phys. Rev. B **41**, 4619 (1990); S. Bacci and E. Gagliano, *ibid.* **43**, 6224 (1991); F. Nori, E. Gagliano, and S. Bacci (unpublished).

[14] R. Rammal and J. Bellisard, J. Phys. (Paris) (to be published).

[15] Y. Y. Wang, B. Pannetier, and R. Rammal, J. Phys. (Paris) **48**, 2067 (1987).

[16] Y.-H. Chen, F. Wilczek, E. Witten, and B. I. Halperin, Int. J. Mod. Phys. B **3**, 1001 (1989).